Journal of
Mechanics of
Materials and Structures

PLASTIC HINGES AS PHASE TRANSITIONS IN STRAIN SOFTENING BEAMS

Gianni Royer-Carfagni and Giovanni Buratti

Volume 2, Nº 9 November 2007

mathematical sciences publishers

JOURNAL OF MECHANICS OF MATERIALS AND STRUCTURES
Vol. 2, No. 9, 2007

PLASTIC HINGES AS PHASE TRANSITIONS IN STRAIN SOFTENING BEAMS

GIANNI ROYER-CARFAGNI AND GIOVANNI BURATTI

A jump between the upper yield point and lower yield point is well evident in strain driven tests on low-carbon steel bars. However, in the constitutive equations commonly used to model the elastic-plastic flexure of beams this jump is usually neglected. Here, we show instead that such jump, albeit small, may drastically vary the structural response, because it renders the moment-curvature relationship of the beam strain-softening in type and with horizontal asymptotes. Because of this, with a process analogous to a phase transition within the solid state itself, strain may suddenly localize in the form of concentrated rotations of the beam axis, indeed forming a *plastic hinge* in the classical sense of limit analysis. Therefore, the formation of plastic hinges, usually indicated as an approximate or technical model, is now rigorously predicted by this approach. Experimental observations corroborate this finding.

1. Introduction

The elastic-plastic design of civil structures is classically associated with the *plastic-hinge* model which allows the technical analysis of the bending of beams in a relatively simple manner. Following this rationale, when a beam made of a ductile material, such as steel, is gradually loaded, plastic hinges are assumed to develop at those sections where the bending moment reaches a certain threshold, that is, at those sections rotations of any amount may occur while the bending moment remains fixed at the threshold value [Neal 1963]. However, the plastic hinge model is traditionally considered an approximate or technical model because, even when the material is idealized as elastic-perfectly plastic, regardless of the shape of beam cross-section the bending moment M is a monotonically increasing function of the beam curvature χ asymptotically approaching, but never reaching, the full plastic moment as $\chi \to \infty$. Thus, the development of a plastic hinge can be read as a borderline case, never attained in practice, but a very useful simplification in the structural analysis.

There are, however, some interesting but perhaps forgotten old experiments by Nakanishi et al. [1934], which have provided a wealth of evidence describing how the plastic hinge model may indeed be more accurate than expected. To illustrate, Figure 1 represents the bending moment $\bar{M}$ versus sag δ relationship measured from tests on simple supported beams with various cross-sections, loaded as in Figure 2. If the material is considered elastic-perfectly plastic and, according to the Bernoulli–Navier hypothesis, cross-sections remain planar in the deformation, then the flexure is uniform in the central portion A-B of Figure 2, and the bending moment is a monotonically increasing function of the beam curvature χ, asymptotically approaching the full plastic threshold. However, this trend is not confirmed by experiments. In fact, if the flexure were uniform, the $\bar{M}$-δ diagrams of Figure 1 would also represent, by a

Keywords: limit analysis, phase transition, strain localization, plastic hinge, nonconvex minimization, holonomic plasticity.
This work is part of the research activities of the EU Network *Phase Transitions in Crystalline Solids*, and is partially supported by the Italian *Ministero per l'Università e la Ricerca Scientifica e Tecnologica* under the program PRIN 2005.

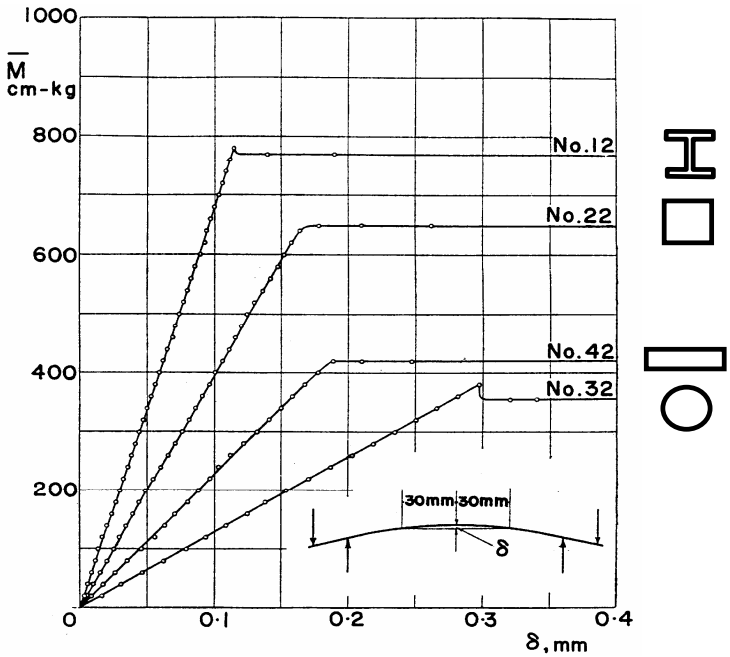

Figure 1. Experimental $\bar{M}$-δ relationships for beams with different cross-sections [Nakanishi et al. 1934].

proper change of scale, the moment-curvature response of the beam. This is because the curvature of its centroid line could be expressed, with the usual first-order approximation, as

$$\chi(z) \cong \frac{8\delta}{l^2}. \tag{1}$$

Quite surprisingly, the graphs of Figure 1 do not show monotonically increasing curves, but rather exhibit a horizontal *plateau*, revealing that the bending moment remains constant while the beam sag increases indefinitely as if a classical *plastic hinge* had developed.

In order to solve the apparent discrepancy between theoretical predictions and experimental results, we simply propose to consider in the constitutive stress-strain law the jump between the so called *upper yield*

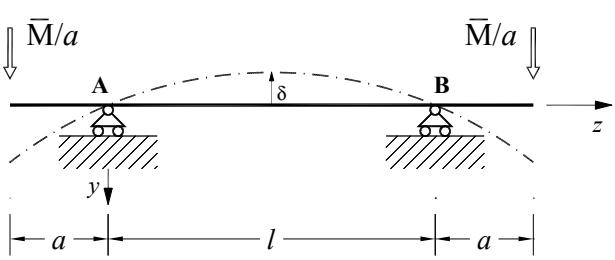

Figure 2. Layout of the experimental configuration for tests of Figure 1 [Nakanishi et al. 1934].

point (Oberestreckgrenze) and *lower yield point* (Unterestreckgrenze). Such jump is usually neglected in the constitutive equations, although it is well evident in strain driven tests on low-carbon steel bars [Neal 1963]. For example, in Figure 3, which shows the engineering stress σ versus the engineering strain ε diagrams as measured in one of the tests recorded in [Froli and Royer-Carfagni 1999], the ratio between *Oberestreckgrenze* and *Unterestreckgrenze* is of the order of 1.12; this value may vary according to the carbon level in the steel. In fact, at the nanoscale, the stress drop can be attributed to the pinning of the dislocations (Peierls–Nabarro effect) due to the presence of solute atoms of carbons in the metallic lattice [Cottrell 1953]. It has been demonstrated [Froli and Royer-Carfagni 2000] that the consideration of such a jump is of crucial importance for the orderly formation, at the microscale, of slip (Lüder) bands in stretched bars of mild steel.

For the case of bending, consideration of this jump is not without consequences because it renders the elastic-plastic moment-curvature relationship $M(\chi)$ nonmonotone in type. Indeed, the nonmonotone character of $M(\chi)$, analogously to the classical loops in the pressure versus volume isotherms of a Van der Waals fluid, may produce a transition in the beam strain reminiscent of the sudden volume change associated with the transition from the liquid to the vapor phase in the fluid. The extension of Van der Waals model to solids has received much attention recently; see [Müller and Villaggio 1977; Dunn and Fosdick 1980]. The relevant theories, which allow for stress- and deformation-induced phase transitions within the solid state itself, predict discontinuous strain fields in reasonable agreement with the experimental observations. Another characteristic feature of the $M(\chi)$ function that will be deduced from the proposed constitutive σ-ε law, is that it exhibits a horizontal asymptote. Truskinovsky [1996] has perhaps been the first to consider the consequences of assuming constitutive relationships with horizontal *plateaux* for the one-dimensional case of a tensile bar, evidencing the consequent possibility of strain localization, similar in type to the nucleation of passing through a crack.

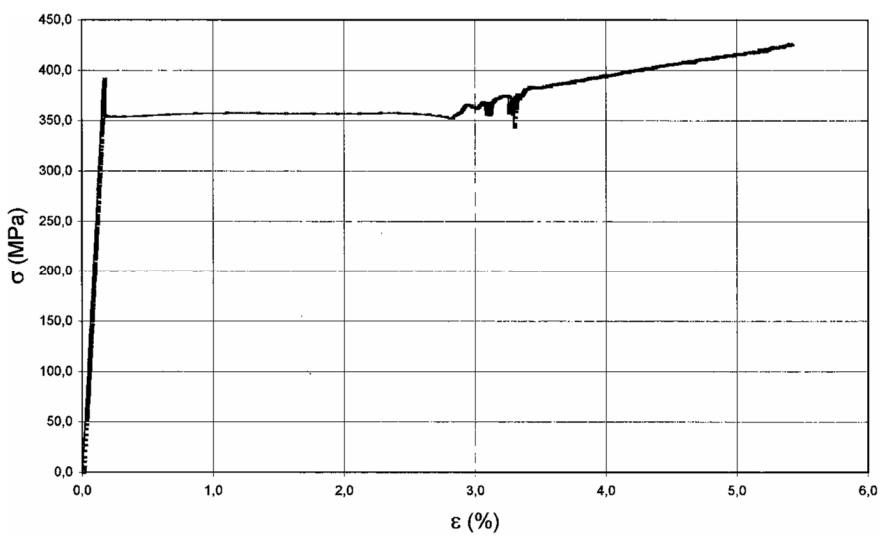

Figure 3. Local σ-ε relationship in a stretched bar of mild steel [Froli and Royer-Carfagni 1999]. Local strain measured with strain gauges.

In this paper we will show that the loops and the horizontal asymptotes of the $M(\chi)$ constitutive law may imply, similarly to phase transitions, a sudden strain localization in the beam, that is, a discontinuity in the rotation field of the centroid line, analogous to the formation of a *plastic hinge* in the classical meaning of limit analysis. An accurate reworking of the traditional technical theories from this novel approach may be of importance, especially in the seismic design of civil engineering works, where the plastic resources in terms of ductility play a decisive role in the structural performance.

2. Moment versus curvature relationships for elastic-plastic beams

To illustrate the consequences of considering a jump between the upper and lower yield points in the stress-strain constitutive law, consider the case of a beam with constant cross-section under flexure. According to the Bernoulli–Navier hypothesis we assume that cross-sections remain planar during bending, so that the elongation of each longitudinal fiber is directly proportional to the distance y from the neutral axis by a coefficient χ, representing the curvature of the centroid line of the beam. In particular, consider the simplest relationship between engineering stress σ and engineering strain ε of the type reported in Figure 4. Clearly, the material is elastic-perfectly plastic, symmetric in tension and compression. Nevertheless, it exhibits a well marked jump from *Oberestreckgrenze* to *Unterestreckgrenze*. For the constitutive law $\sigma(\varepsilon)$ can be written in the form

$$\sigma(\varepsilon) = \begin{cases} -\sigma_0, & \varepsilon < -\varepsilon_0, \\ \alpha \frac{\sigma_0}{\varepsilon_0}\varepsilon, & -\varepsilon_0 \le \varepsilon \le \varepsilon_0, \\ \sigma_0, & \varepsilon > \varepsilon_0, \end{cases}$$

where $\alpha\sigma_0$, with $\alpha > 1$, is the *Oberestreckgrenze* and σ_0 the *Unterestreckgrenze*.

Let us now examine beams with cross-sections of three different shapes. Consider first a rectangular cross section of depth h and width b. As the beam curvature χ is gradually increased, the distribution of normal stress along the depth of the cross-section is of the type sketched in Figure 5, where χ_{I} denotes the curvature corresponding to the elastic limit. When the curvature is increased beyond χ_{I}, the most distant fibers from the neutral axis are strained beyond ε_0 and, consequently, in these overstrained regions

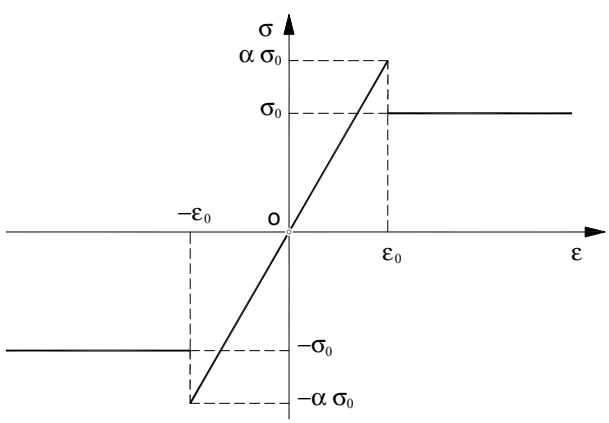

Figure 4. Stress-strain relationship with stress jump at yielding.

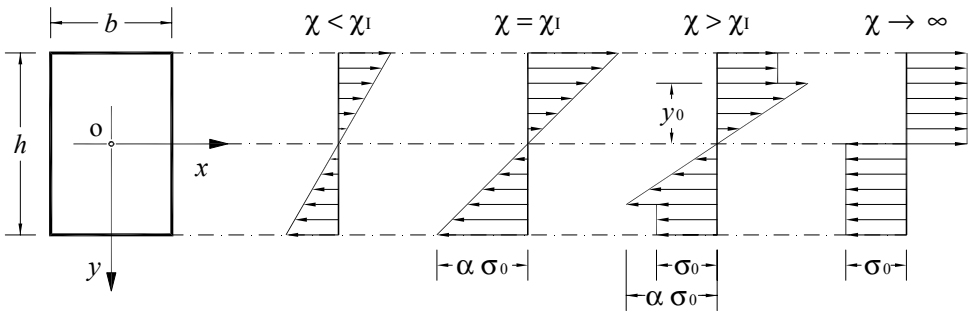

Figure 5. Rectangular cross-section: stress distribution with discontinuous σ-ε relationship.

the stress remains constant and equal to the lower yield point stress, σ_0. Further increasing the curvature, more and more fibers reach the yield point until the entire beam, with the exception of a thin layer at the neutral axis, becomes plastic. In Figure 5 this condition is referred to as the stage $\chi \to \infty$.

Denoting by y_0 the distance from the fiber neutral axis at which the strain reaches the limit value ε_0, the relationship between bending moment and curvature is $M(\chi) = \frac{2}{3}Eby_0^3\chi + \sigma_0 b\left(\frac{1}{4}h^2 - y_0^2\right)$, where

$$y_0 = \begin{cases} h/2, & \chi \le \chi_{\mathrm{I}}, \\ \alpha\sigma_0/(\chi E), & \text{otherwise}, \end{cases}$$

and E denotes the Young's modulus. The corresponding moment-curvature M-χ relationship is represented in Figure 6 for different values of the parameter α. In particular, observe that for $\alpha > 3/2$ the M-χ curve exhibits a well-recognizable strain-softening branch. In this latter case, under a strain history monotonically increasing the curvature χ, the work U consumed in deforming the beam per unit beam length defined as

$$U(\chi) = \int_0^{\chi} M(\eta)d\eta \tag{2}$$

is a nonconvex function with oblique asymptotes of the type schematically represented in Figure 7.

As a second example consider a beam whose cross-section is rhomboidal with depth b_R and height h_R. The stress diagram for gradually increasing curvatures is shown in Figure 8, while the corresponding M-χ relationship is qualitatively sketched in Figure 9. Again, when $\alpha > 3/2$, the bending moment attains

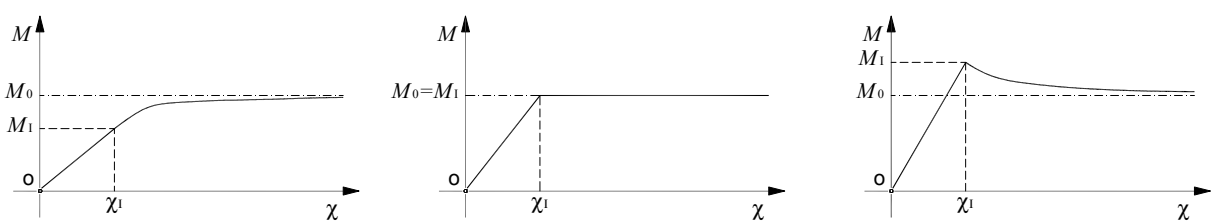

Figure 6. Bending moment versus curvature of beams with rectangular cross-section for (a) $1 < \alpha < 3/2$, (b) $\alpha = 3/2$, (c) $\alpha > 3/2$.

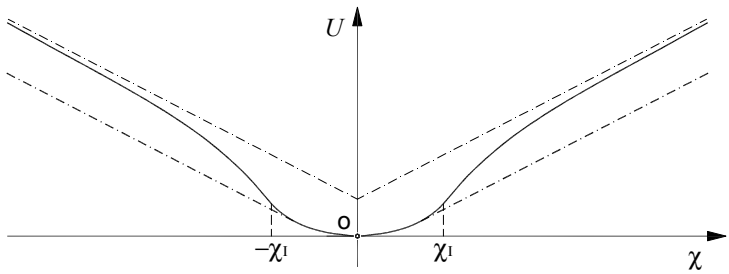

Figure 7. Rectangular cross section. Elastic-plastic work per unit length $U(\chi)$ for $\alpha > 3/2$.

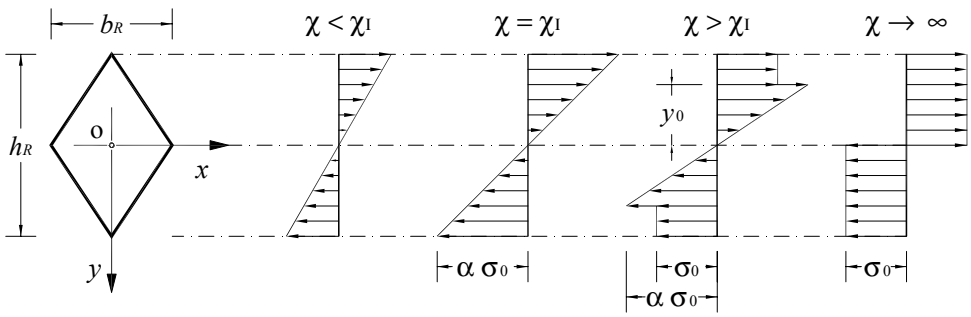

Figure 8. Stress distribution for rhomboidal cross-sections.

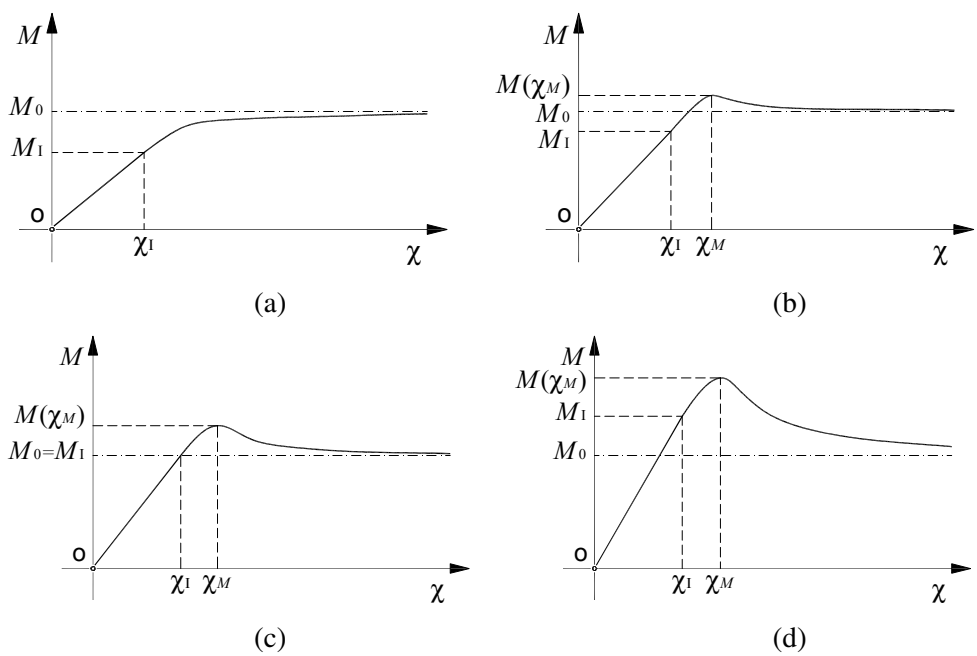

Figure 9. Bending moment versus curvature for rhomboidal cross-sections for (a) $1 < \alpha \leq 3/2$, (b) $3/2 < \alpha \leq 2$, (c) $\alpha = 2$, (d) $\alpha > 2$.

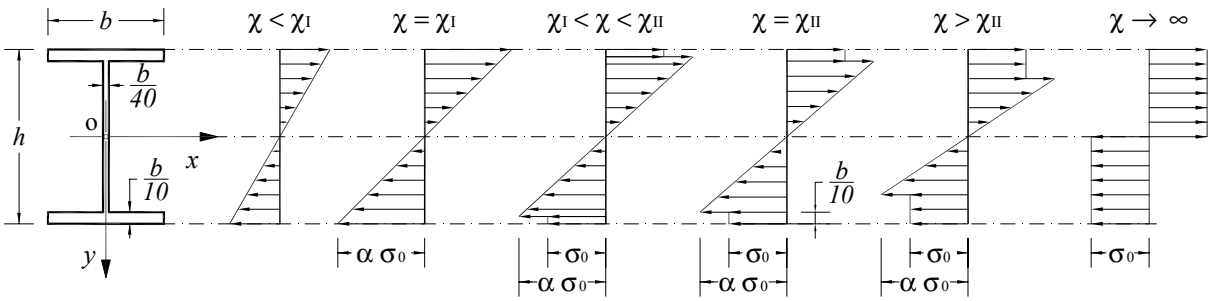

Figure 10. I-shaped cross-section: stress distribution with discontinuous σ-ε relationship.

its maximum value at the (finite) curvature given by

$$\chi_{\mathrm{M}} = \frac{3}{2h_R}\frac{3\alpha-4}{2\alpha-3}, \qquad M(\chi_{\mathrm{M}}) = \frac{(128\alpha^2-333\alpha+216)\alpha}{324(4-3\alpha)^2} b_R h_R^2,$$

but such value is greater than the full plastic moment M_0. Consequently, the $M(\chi)$ curve becomes nonmonotone, with a strain softening branch. Correspondingly, the work consumed in deforming the beam $U(\chi)$ results again in a nonconvex type when $\alpha > 3/2$.

As a third, and perhaps most practically relevant example, consider an I-shaped cross section. The stress-distribution at different values of the curvature is schematically represented in Figure 10, where χ_{I} denotes again the elastic limit curvature and χ_{II} the curvature at which the flanges become plastic.

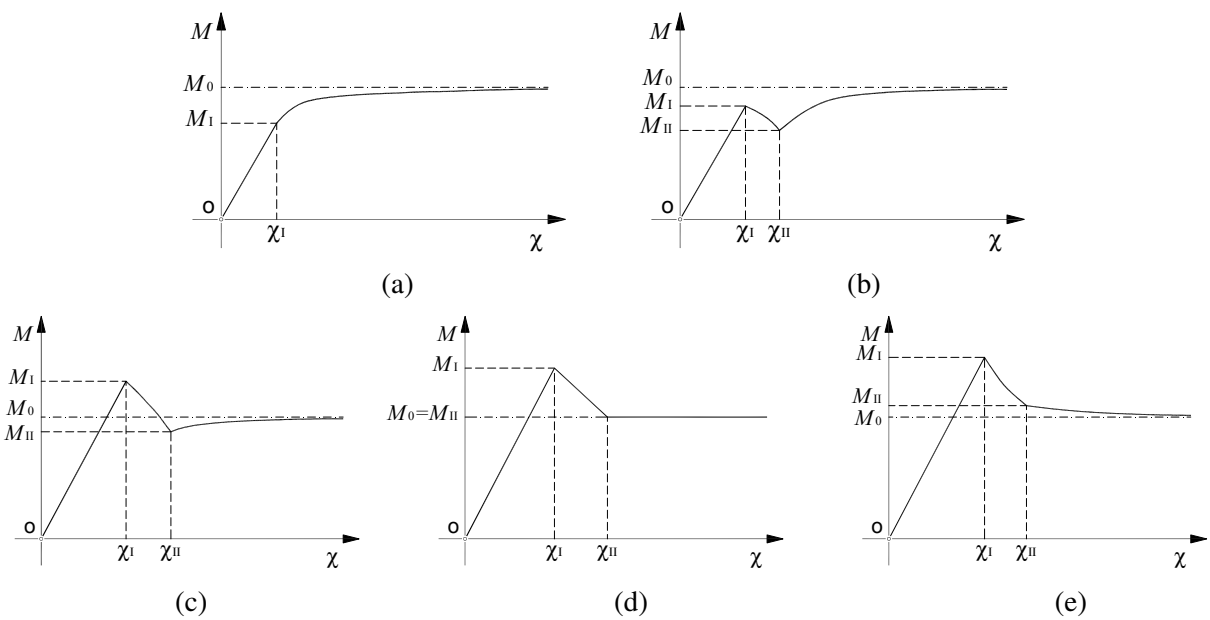

Figure 11. Bending moment versus curvature for I-shaped beams for (a) $\alpha \le 60/59$, (b) $60/59 < \alpha \le 12615/11569$, (c) $12615/11569 < \alpha < 3/2$, (d) $\alpha = 3/2$, (e) $\alpha > 3/2$.

The M-χ curves obtained for different choices of the parameter α are schematically represented in Figure 11. Remarkably, in the third example the dependence of the M-χ relationship on α is quite nonlinear, and the nonmonotone character is observed also for very small values of α. This finding is crucial for the forthcoming analysis, where a nonmonotone (strain-softening) character for the moment-curvature relationship will be systematically assumed. The corresponding diagrams for the elastic-plastic work $U(\chi)$ are sketched in Figure 12.

Note that in this case the nonmonotone character of the bending M-χ relationship is attained also for small jumps in the stress-strain curve, specifically for $\alpha > 60/59$. A value of this order is certainly reached in practice; experimental tests on mild steel show that $\alpha \cong 1.1$ [Froli and Royer-Carfagni 1999]. Moreover, as the parameter α is varied within this range, the corresponding graphs of $M(\chi)$ and $U(\chi)$ may exhibit loops that are different in kind. Thus, at least for I-shaped profiles, the discussion of the cases when the moment-curvature relationship is of the type represented in Figure 11 acquires a practical interest.

3. The energy functional

Consider a simply supported beam subject to a transversally distributed load $q(z)$ and two couples, W_A and W_B, acting at its ends (considered positive if oriented as in Figure 13). Let $v(z)$ denote the displacement component in the y-direction of the beam centroid axes at z, $\varphi(z)$ the corresponding rotation which is positive if counterclockwise, and define the curvature χ through the relationship $\chi(z) = \varphi'(z)$, where the prime indicates a derivative with respect to z.

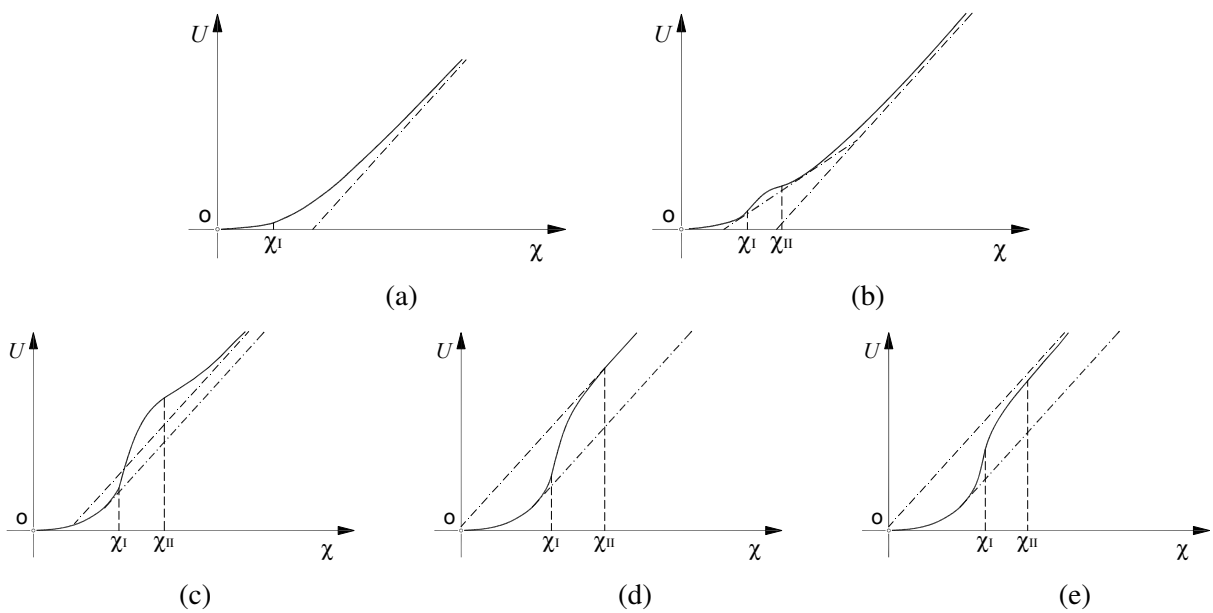

Figure 12. Elastic-plastic work per unit length $U(\chi)$ in I-shaped beams for (a) $\alpha \le 60/59$, (b) $60/59 < \alpha \le 12615/11569$, (c) $12615/11569 < \alpha < 3/2$, (d) $\alpha = 3/2$, (e) $\alpha > 3/2$.

At this stage, the analysis will be limited to the case of holonomic plasticity only, so that a strain energy functional can be defined. This produces noteworthy simplifications because the beam stable equilibrium configurations will be associated with absolute minimizers of the energy functional. This allows modern techniques in the calculus of variations to be applied to the corresponding nonconvex minimization problem. Under these assumptions, the energy functional associated with the sum of the strain energy and the potential energy of the applied loads can be written in the form

$$E[\varphi, v] = \int_0^L U\big(\varphi'(z)\big)dz - \int_0^L q(z)v(z)dz - \big[W\varphi(z)\big]_{z=0}^{z=L}, \tag{3}$$

where $U(\varphi') = U(\chi)$ is the bulk energy density, defined as in Equation (2). In general, for the reasons discussed in Section 2, U is an even, nonconvex function whose qualitative form will represented by one of the graphs in Figure 12.

It is useful to introduce the quantity

$$T(z) = -\int_0^z q(z)dz + C_1, \tag{4}$$

where C_1 is a constant whose value will be determined afterward. It is easy to recognize that when the constant C_1 represents the vertical reaction at point A of Figure 13, then $T(z)$ denotes the shear force acting at section z. The importance of Equation (4) is that it allows us to write a convenient expression for the work of the external load. In fact, by setting

$$\varphi(z) \cong -\frac{d}{dz}v(z) \tag{5}$$

as customary in the technical theory of beams, upon integrating by parts one obtains

$$\int_0^L q(z)v(z)dz = \int_0^L T(z)v'(z)dz - \big[T(z)v(z)\big]_{z=0}^{z=L} = -\int_0^L T(z)\varphi(z)dz, \tag{6}$$

that, once introduced into Equation (3), provides a simpler form of the total energy functional to be minimized. In particular,

$$\pi[\varphi] = \int_0^L U\big(\varphi'(z)\big)dz + \int_0^L T(z)\varphi(z)dz - \big[W(z)\varphi(z)\big]_{z=0}^{z=L}, \tag{7}$$

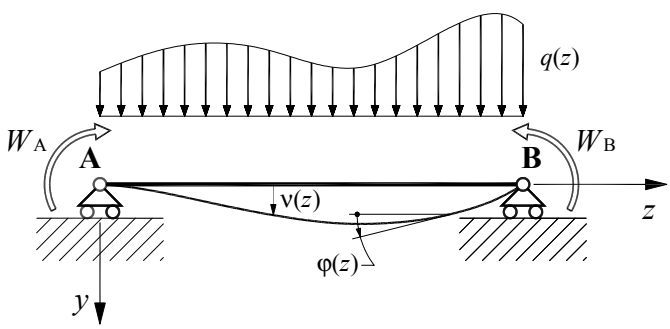

Figure 13. Generic layout of beam under flexure.

since now only the rotation field φ comes into play. Using Equation (5) the boundary conditions $v(0) = v(L) = 0$ can be equivalently restated in terms of φ only via

$$\int_0^L \varphi(z)dz = 0. \tag{8}$$

Solutions of the variational problem have to be sought in the space of function of bounded variation on $[0, L]$, usually referred to as $BV[0, L]$. For our derivations we will need to use some notions of functional analysis; see [Kolmogorov and Fomin 1975] for details and notation. The necessity of considering a space of functions allowing for discontinuities such as the space BV comes essentially from the presence of the oblique asymptotes in the strain energy function $U(\chi)$. In fact, due to the linear growth of $U(\chi)$ at infinity, a finite value of the energy is associated with infinite curvatures.

To illustrate this point, let us take a step function of the type

$$H(z) = \begin{cases} 0, & 0 \le z < z_0, \\ \varphi_0, & z_0 \le z \le L, \end{cases}$$

where φ_0 is a fixed number. Consider then the sequence $\varphi^H_{(n)}(z)$ defined by

$$\varphi^H_{(n)}(z) = \begin{cases} 0, & 0 \le z < z_0, \\ \varphi_0\, n(z - z_0), & z_0 \le z \le z_0 + 1/n, \\ \varphi_0, & z_0 < z \le L, \end{cases}$$

converging to $H(z)$ when $n \to \infty$. The derivative of $\varphi^H_{(n)}(z)$ with respect to the variable z is not null in the interval $z_0 \le z \le z_0 + 1/n$ only, where it is constant and directly proportional to n. But $U(\varphi'(z))$ has oblique asymptotes with slope $\pm M_0$; consequently, the strain energy remains bounded also when $n \to \infty$ because

$$\lim_{n\to\infty} \int_0^L U\big(\varphi^{H\prime}_{(n)}(z)\big)dz \cong \lim_{n\to\infty} \left(\mathrm{sgn}(\varphi_0)\mathrm{M}_0 \frac{\varphi_0}{1/\mathrm{n}} \frac{1}{\mathrm{n}}\right) = \mathrm{M}_0\, \varphi_0\, \mathrm{sgn}(\varphi_0) = \mathrm{M}_0|\varphi_0|, \tag{9}$$

where $\mathrm{sgn}(\varphi_0)$ denotes the sign of φ_0. Therefore, since by Equation (9) the total energy is also limited for functions with discontinuous rotation fields, the possibility of discontinuities must be contemplated in a proper class of function in which minimizers have to be sought. Moreover, the energy functional given in Equation (3) must be modified to account for the energy associated with the singularities of the rotation field.

The energy contribution due to concentrated rotations has been evaluated with a limit procedure by Royer-Carfagni [2001]. Here we only recall the main results, which were also discussed in [Del Piero 2003]. First of all, recall by Lebesgue decomposition [Kolmogorov and Fomin 1975] that any function φ of bounded variation can written in the form

$$\varphi(\cdot) = \varphi_a(\cdot) + \varphi_s(\cdot) + \varphi_d(\cdot), \tag{10}$$

that is, the sum of a function φ_a whose derivative, in the sense of distributions, is absolutely continuous with respect to the Lebesgue measure, a singular Cantor-like function φ_s and a jump function φ_d. Then, the new energy functional $\Pi[\varphi]$ to be considered [Royer-Carfagni 2001] has the property that $\Pi[\varphi]$

coincides with $\pi[\varphi]$ of Equation (7) whenever $d\varphi(z)$ is absolutely continuous, that is, $d\varphi_s = d\varphi_d \equiv 0$. Furthermore, $\liminf_{n\to\infty} \pi[\varphi_{(n)}] = \Pi[\varphi]$ for any sequence $\varphi_{(n)}$ converging in a suitable topology [1] onto a singular function φ with null absolutely continuous part, that is, with $\varphi_a \equiv 0$.

The result is as follows. Recalling that any function in BV: $\mathbb{R} \to \mathbb{R}$ can be written as the sum of a nondecreasing function and a nonincreasing function [Kolmogorov and Fomin 1975], using Equation (6) and writing φ_s as the sum of a nondecreasing and nonincreasing functions φ_s^+ and φ_s^- acting in their domains of definition J_+ and J_-, respectively, the energy stored in the beam, obtained by augmenting Equation (3) of the contribution due to possible irregularities in the rotation field, can be written in the form [Royer-Carfagni 2001; Del Piero 2003]

$$\Pi[\varphi] = \int_0^L U(\varphi_a')dz + M_0\Big(\int_{J_+} d\varphi_s^+ - \int_{J_-} d\varphi_s^-\Big) + M_0 \sum_{z\in\Gamma(\varphi)} \big|[\![\varphi]\!](z)\big| + \int_0^L T(z)\varphi(z)dz - \big[W(z)\varphi(z)\big]_{z=0}^{z=L}, \quad (11)$$

where $\Gamma(\varphi)$ is the (countable) set of discontinuity points of φ and $[\![\varphi]\!](z) := \varphi(z^+) - \varphi(z^-)$ is the jump of φ at $z \in \Gamma(\varphi)$. It should be remarked that in addition to a bulk term Equation (11) also consists of a surface or interfacial part, that is, the part associated with the Cantor part $d\varphi_s$ and jump part $[\![\varphi]\!]$ of φ. Such parts take into account of the energy consumed at those points where the beam curvature becomes infinite.

The energy functional has to be minimized in the class $\varphi \in BV[0, L] \to \mathbb{R}$ subject to the condition

$$\int_0^L \varphi(z)dz = \int_0^L \varphi_a(z)dz + \int_0^L \varphi_s(z)dz + \int_0^L \varphi_d(z)dz = 0, \quad (12)$$

analogous to Equation (8). In what follows, we will consider the variational problem of minimizing $\Pi[\varphi]$ for two specific cases.

4. Simple supported beam under uniform bending

Consider first the bending of an originally straight beam loaded by bending moments at its ends, that is, $W(z = 0) = W_A$, $W(z = L) = W_B$ and $q(z) \equiv 0$ in the notation of Figure 13. To analyze the stationary points of the energy functional Equation (11), observe first that $q(z) = 0$ and Equation (6) imply $\int_0^L T(z)\varphi(z)dz = 0$. Let then $\varphi^*(z) \in BV : [0, L] \to \mathbb{R}$ be a minimizer of $\Pi[\varphi]$ of Equation (11), and consider the variation $\varphi^* + \varepsilon\psi$. Lebesgue's decomposition (10) gives

$$\psi = \psi_a + \psi_s + \psi_d \in BV : [0, L] \to \mathbb{R}, \quad (13)$$

with $d\psi$ consisting of the absolutely continuous part $d\psi_a$, the singular part $d\psi_s$ and the jump part $d\psi_d$. Then, by the boundary condition (8), ψ has to satisfy

$$\int_0^L \psi(z)dz = \int_0^L \psi_a(z)dz + \int_0^L \psi_s(z)dz + \int_0^L \psi_d(z)dz. \quad (14)$$

[1] The weak* topology in the space of measures [Buttazzo 1989].

The necessary conditions for equilibrium, yielded by a standard procedure of calculus of variation, are given by the inequality

$$\lim_{\varepsilon\to 0^+} \frac{\Pi[\varphi^* + \varepsilon\psi] - \Pi[\varphi^*]}{\varepsilon} \geq 0, \qquad \text{for all } \psi. \tag{15}$$

For the following, it is convenient to introduce the function

$$M^*(z) = U'\big(\varphi_a^{*\prime}(z)\big), \tag{16}$$

representing the bending moment in the beam. Three classes of perturbations will be considered.

In the first case, let $d\psi = d\psi_a$, $d\psi_s = d\psi_d = 0$, that is, the perturbation is represented by a rotation field whose distributional derivative is absolutely continuous with respect to the Lebesgue measure. Since two-sided variations are allowed, the inequality (15) reduces to the equality

$$0 = d\Pi[\psi] = \int_0^L U'\big(\varphi_a^{*\prime}(z)\big)\psi_a'(z)dz - \big[W(z)\psi_a(z)\big]_{z=0}^{z=L},$$

that, after integrating by parts and using Equation (16), can be rewritten in the form

$$\begin{aligned} 0 = d\Pi[\psi] &= \big[U'\big(\varphi_a^{*\prime}(z)\big)\psi_a(z)\big]_{z=0}^{z=L} - \int_0^L \frac{d}{dz}U'\big(\varphi_a^{*\prime}(z)\big)\psi_a(z)dz - \big[W(z)\psi_a(z)\big]_{z=0}^{z=L} \\ &= -\int_0^L \frac{d}{dz}M^*(z)\psi_a(z)dz + \big[\big(M^*(z) - W(z)\big)\psi_a(z)\big]_{z=0}^{z=L}. \end{aligned} \tag{17}$$

Because of the arbitrariness of ψ_a and Equation (14), this is satisfied if and only if

$$-\frac{d}{dz}M^*(z) = C = \text{const}, \qquad M^*(z=0, L) = W(z=0, L). \tag{18}$$

These are the standard equilibrium equations at the interior points and at the ends of the beam, respectively. Consequently, integrating the first equation of (18), with the natural conditions given in the second part of (18) one gets

$$M^*(z) = \frac{W_{\mathrm{B}} - W_{\mathrm{A}}}{L}z + W_{\mathrm{A}}. \tag{19}$$

In the particular case of uniform bending whence $W_{\mathrm{A}} = W_{\mathrm{B}}$ as in Figure 2, Equation (19) reduces to

$$M^*(z) = W_{\mathrm{A}}. \tag{20}$$

As a second case, consider the variation $d\psi = d\psi_a + d\psi_s$, $d\psi_d = 0$. Condition (15) yields

$$\int_0^L M^*(z)\psi_a'(z)dz + M_0\Big(\int_{J_+} d\psi_s - \int_{J_-} d\psi_s + \int_{J_0} |d\psi_s|\Big) - \big[W(z)\psi(z)\big]_{z=0}^{z=L} \geq 0, \tag{21}$$

with $J_0 = \mathrm{Supp}[d\psi_s]\backslash\{J_+ \cup J_-\}$, where $\mathrm{Supp}[d\psi_s]$ denotes the support of $d\psi_s$. Consequently, integrating by parts the first integral and recalling that $\psi_a = \psi - \psi_s$, we get

$$-\int_0^L \frac{d}{dz}M^*(z)\psi(z)dz + \int_0^L \frac{d}{dz}M^*(z)\psi_s dz + \big[M^*(z)\psi_a(z)\big]_{z=0}^{z=L} + M_0\Big(\int_{J_+} d\psi_s - \int_{J_-} d\psi_s + \int_{J_0} |d\psi_s|\Big) - \big[W(z)\psi(z)\big]_{z=0}^{z=L} \geq 0. \quad (22)$$

However, from the conditions (14) and (18) the first term vanishes. Thus, integrating by parts once more and using Equation (18), Equation (22) can be put into the equivalent form

$$-\int_0^L M^*(z)d\psi_s + M_0\Big(\int_{J_+} d\psi_s - \int_{J_-} d\psi_s + \int_{J_0} |d\psi_s|\Big) + \big[\big(M^*(z) - W(z)\big)\psi(z)\big]_{z=0}^{z=L} = -\int_0^L M^*(z)d\psi_s + M_0\Big(\int_{J_+} d\psi_s - \int_{J_-} d\psi_s + \int_{J_0} |d\psi_s|\Big) \geq 0.$$

From this inequality, after subdividing the first integral into the same portions, J_+, J_- and J_0 and using the arbitrariness of $d\psi_s$, one gets the following conditions

$$\begin{aligned} &M(z) = M_0, && \text{for all } z \in J_+,\\ &M(z) = -M_0, && \text{for all } z \in J_-,\\ &-M_0 \leq M(z) \leq M_0, && \text{for all } z \in J_0. \end{aligned} \quad (23)$$

In words, the bending moment cannot take values outside the interval $[-M_0, M_0]$. Moreover, where the rotation field presents positive or negative discontinuities, the bending moment must be equal to M_0 or $-M_0$, respectively.

Finally, assume a perturbation $d\psi = d\psi_a + d\psi_d$, $d\psi_s = 0$, such that the term ψ_d satisfies the condition

$$\psi_d = \begin{cases} 0, & 0 \leq z < z_0,\\ [\![\psi_d]\!](z_0) \neq 0, & z_0 \leq z < L. \end{cases} \quad (24)$$

If $[\![\varphi^*]\!](z_0) = 0$ one obtains $\int_0^L M^*(z)\psi_a'(z)dz + M_0|[\![\psi_d]\!](z_0)| - [W(z)\psi(z)]_{z=0}^{z=L} \geq 0$, that, due to Equations (14) and (18), similarly to the second case, can be rewritten as

$$\begin{aligned} -\int_0^L M^*(z)d\psi_d + \big[M^*(z)\psi_d(z)\big]_{z=0}^{z=L} + \big[M^*(z)\psi_a(z)\big]_{z=0}^{z=L} + M_0\big|[\![\psi_d]\!](z_0)\big| - \big[W(z)\psi(z)\big]_{z=0}^{z=L}\\ = -M^*(z_0)[\![\psi_d]\!](z_0) + M_0\big|[\![\psi_d]\!](z_0)\big| + \big[\big(M^*(z) - W(z)\big)\psi(z)\big]_{z=0}^{z=L}\\ = -M^*(z_0)[\![\psi_d]\!](z_0) + M_0\big|[\![\psi_d]\!](z_0)\big| \geq 0, \end{aligned}$$

giving the condition $-M_0 \leq M^*(z_0) \leq M_0$. Otherwise, if $[\![\varphi^*]\!](z_0) \neq 0$, one finds

$$\int_0^L M^*(z)\psi_a'(z)dz + M_0\big([\![\psi_d]\!](z_0)\big)\mathrm{sgn}\big([\![\varphi^*]\!](z_0)\big) - \big[W(z)\psi(z)\big]_{z=0}^{z=L} \geq 0.$$

Consequently, $-M^*(z_0)[\![\psi_d]\!](z_0) + M_0\big([\![\psi_d]\!](z_0)\big)\mathrm{sgn}\big([\![\varphi^*]\!](z_0)\big) \geq 0$. Since $[\![\psi_d]\!](z_0)$ is arbitrary, this is equivalent to the condition

$$M^*(z_0) = M_0\mathrm{sgn}\big([\![\varphi^*]\!](z_0)\big), \tag{25}$$

from which it follows that at the jump points of φ^* the function M^* can assume the values M_0 or $-M_0$. The sign of the bending moment is consistent with the sign of the jump, as stated by Equation (25).

The analysis of the second variation for the energy functional (11) provides the simple inequality

$$U''\big(\varphi_a^{*\prime}\big) \geq 0. \tag{26}$$

It is then clear that any field that solves the Euler equations, but attains the softening branches of the moment curvature relationship, that is, the concave portion of the strain potential, corresponds to an *unstable* equilibrium configuration.

Finally, for a complete characterization of minimizers it is convenient to introduce an auxiliary problem known as the relaxed problem. After a well known procedure in the calculus of variations [Buttazzo 1989], the relevant procedure consists of the minimization of the *relaxed* strain energy functional

$$\Pi^{**}[\varphi] = \int_0^L U^{**}(\varphi_a')dz + M_0\Big(\int_{J+} d\varphi_s^+ - \int_{J-} d\varphi_s^-\Big) + M_0 \sum_{z\in\Gamma(\varphi)} \big|[\![\varphi]\!](z)\big| + \int_0^L T(z)\varphi(z)dz - \big[W(z)\varphi(z)\big]_{z=0}^{z=L}. \tag{27}$$

This functional is identical to $\Pi[\varphi]$ of Equation (11) except for the strain energy density U that has been substituted with its lower-convex envelope U^{**}, that is, the lower convex function which supports U from below. Observe that U^{**} is identified by the envelope of the lines that are tangent but not intersecting the graph of U and, for the cases shown in Figure 12, such envelope is delimited by those tangent lines which are parallel to the oblique asymptotes of U. Correspondingly, the graph of $U^{**\prime}$ presents a *horizontal plateau* in correspondence with the horizontal asymptote of U'.

As discussed at length by Royer-Carfagni [2001], the relationship between the original energy (11) and the relaxed energy (27) consists of the fact that minimizers $\varphi^*$of $\Pi[\varphi]$ enjoy the properties that $U^{**}(\varphi_a^{*\prime}(z)) \equiv U(\varphi_a^{*\prime}(z))$, $\forall z \in (0, L)$. In other words, the beam curvature $\chi^*(z) \equiv \varphi_a^{*\prime}(z)$ can only attain those values at which U coincides with its lower convex envelope U^{**}. This finding, first observed by Truskinovsky [1996], represents the natural extension to localized deformations of the well known Ericksen's problem of a tensile bar with nonconvex strain energy [Ericksen 1975]. In conclusion, solutions of the nonconvex minimization problem can be equivalently investigated by considering the associated *relaxed* minimization problem that, in the one-dimensional case, is obtained by substituting the strain energy function with its lower convex envelope.

In order to characterize the equilibrium states of the beam, one has to consider the conditions (18), (23) and (25). One of the main results due to Equation $(23)_3$, is that deformation paths made of stable equilibrium configurations cannot attain values of the bending moment outside the interval $[-M_0, M_0]$, whose extremities are defined by the levels of the horizontal asymptotes of the moment-curvature relationship. For the cases represented in Figure 11 it follows, in particular, that those parts of the linear elastic path passing through the origin that are outside the interval $[-M_0, M_0]$ are inaccessible via stable configurations and should be regarded as points of metastable equilibrium.

Now, let a beam be gradually strained according to the static scheme of Figure 2, corresponding to the Nakanishi experimental condition referred to in Section 1. The central portion A-B of the beam is uniformly bent, that is, $W_A = W_B \equiv \bar{M}$ and $q = 0$ in the scheme of Figure 13, so that Equation (20) holds. Imagine now that a closed loop control of the loading device allows to gradually increase the sag δ by controlling applied force $\bar{M}/a$ of Figure 2 (strain driven test), and consider the beam response for various forms of the M-χ constitutive relationships, of the type represented in Figure 11.

Consider first the case of part (a) of Figure 11, where the M-χ law is strain-hardening in type and the associated strain potential strictly convex. Then, whenever $\bar{M} < M_0$, by Equation (23) the rotation field $\varphi^*(z)$ must be absolutely continuous, that is, $\varphi_s^*(z) = \varphi_d^*(z) \equiv 0$. Consequently, the curvature is uniform and, by Equation (1), a unique value of the sag δ corresponds to each value of $\bar{M}$. According to Equation (25), strain localization in the form of concentrated rotations may occur when $\bar{M}$ reaches the threshold value M_0, but before reaching such a value the beam curvature has to become, at least in theory, infinite. In other words, whenever the constitutive relationship M-χ is monotonically increasing, the beam is bent with uniform curvature. Consequently, because of Equation (1), the experimental tests of Figure 1 should provide a M versus δ response that should be similar, at the qualitative level, to the M versus χ graph of Figure 11 in part (a). However, Nakanishi's results do not corroborate this finding.

As a second case, assume that the constitutive law of the bar is the one of part (b) of Figure 11. What should be observed now is that whenever the bending moment $\bar{M}$ satisfies $M_{\mathrm{II}} < \bar{M} < M_{\mathrm{I}}$, there are three values of the curvature that correspond to the same value of $\bar{M}$. In this situation, the characterization of minimizers is analogous to that recorded by James and Fosdick [1981], even if the energy they considered, though nonconvex, exhibited a superlinear growth at infinity that prevented the formation of singularities in the minimizing field. Introducing the Maxwell line $M = M_{\mathrm{M}}$ in the graph of the function $M(\chi)$ determined by the equal area rule as in part (a) of Figure 14 and the lower convex envelope of the potential $U(\chi)$ as in part (b), and recalling Equation (1), the $\bar{M}$-δ relationship resulting from the corresponding nonconvex minimization problem takes the form

$$\bar{M} = \begin{cases} M(8\delta/l^2), & \delta \le \delta_{\mathrm{A}} = \chi_{\mathrm{A}} l^2/8, \\ M_{\mathrm{M}}, & \delta_{\mathrm{A}} \le \delta \le \delta_{\mathrm{B}} = \chi_{\mathrm{B}} l^2/8, \\ M(8\delta/l^2), & \delta \ge \delta_{\mathrm{B}} = \chi_{\mathrm{B}} l^2/8. \end{cases}$$

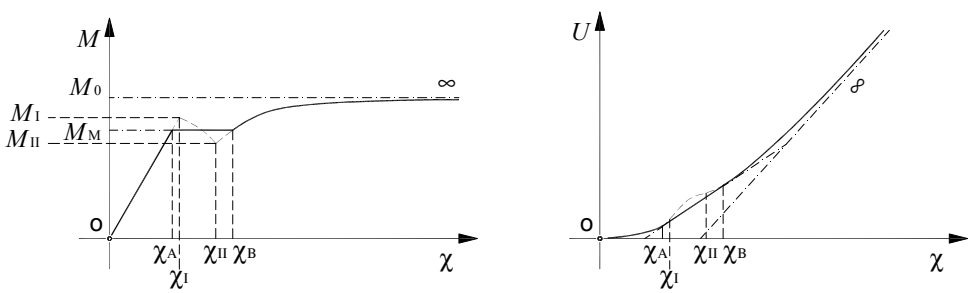

(a) (b)

Figure 14. Equilibrium configuration path for case (b) in Figure 11: (a) M-χ relationship, (b) U-χ relationship.

In particular, similarly to phase transitions [Ericksen 1975], provided the test is strain driven, when $\bar{M} = M_{\mathrm{M}}$ the beam curvature may take the constant value $\chi = \chi_{\mathrm{A}}$ on a portion of length l_A and the constant value $\chi = \chi_{\mathrm{B}}$ on a portion of length $l_B = l - l_A$ satisfying $8\delta_A/l \le \chi_{\mathrm{A}} l_A + \chi_{\mathrm{B}} l_B \le 8\delta_B/l$. Consequently, the $\bar{M}$-δ response exhibits a plastic plateau in correspondence of the Maxwell line, followed by a work-hardening branch. Likewise, in the previous case, by Equation (25) concentrated rotations may develop when $\bar{M}$ approaches M_0, but only after that the beam curvature has attained very large uniform curvatures. However, this response again does not match the experimental results of Figure 1.

The situation becomes more involved when the moment-curvature relationship $M(\chi)$ is as in part (c) of Figure 11. Clearly, when $\bar{M} \le M_{\mathrm{II}}$ to each value of the bending moment corresponds one and only one value of the beam curvature. Therefore, the central portion A-B of Figure 2 becomes uniformly bent and, by Equation (1), the corresponding sag ends up being $\delta = M^{-1}(\bar{M})l^2/8$. Moreover, by Equation (23) one finds that stable equilibrium states must satisfy $0 \le \bar{M} \le M_0$. Consequently, any equilibrium configuration attaining the branches with $\bar{M} \ge M_0$ has to be considered metastable.

It should be noticed, however, that when $M_{\mathrm{II}} \le \bar{M} \le M_0$ there are still three different values of the curvature which correspond to the same value of the applied bending moment. On the one hand, the second variation condition (26) rules out the possibility of attaining the strain softening branch, which corresponds to unstable equilibrium states. On the other hand, it is possible to find equilibrium states for which the beam curvature takes two distinct values, one in the interval $(\chi_{\mathrm{I}} M_{\mathrm{II}}/M_{\mathrm{I}}, \chi_{\mathrm{I}} M_0/M_{\mathrm{I}})$, that is, on the first linear elastic branch, the other in the strain hardening branch $(\chi_{\mathrm{II}}, +\infty)$, both corresponding to the same value of the bending moment $\bar{M}$. In order to recognize if such states are of stable equilibrium, it is necessary to consider the relaxed problem and the minimization of the relaxed energy (27), obtained by introducing the lower convex envelope of the strain energy $U(\chi)$ in part (c) of Figure 12. The lower convex envelope is represented with bold face in part (b) of Figure 15 and the corresponding moment-curvature relationship $M(\chi)$, which follows the Maxwell line at $M = M_0$, in part (a) of Figure 15. The result is that curvatures attaining the branch $(\chi_{\mathrm{II}}, +\infty)$ do not correspond to minimizers because $U(\chi) \ne U^{**}(\chi)$ when $\chi \in (\chi_{\mathrm{II}}, +\infty)$ [Royer-Carfagni 2001]. In particular, Royer-Carfagni [2001] demonstrated that it would be possible to lower the energy by considering curvature in the branch $(0, \chi_A)$.

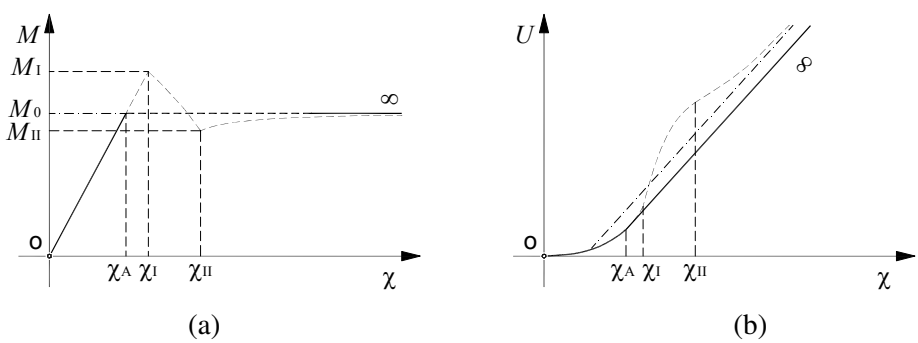

Figure 15. Equilibrium configuration path for case (c) of Figure 11: (a) M-χ relationship, (b) U-χ relationship.

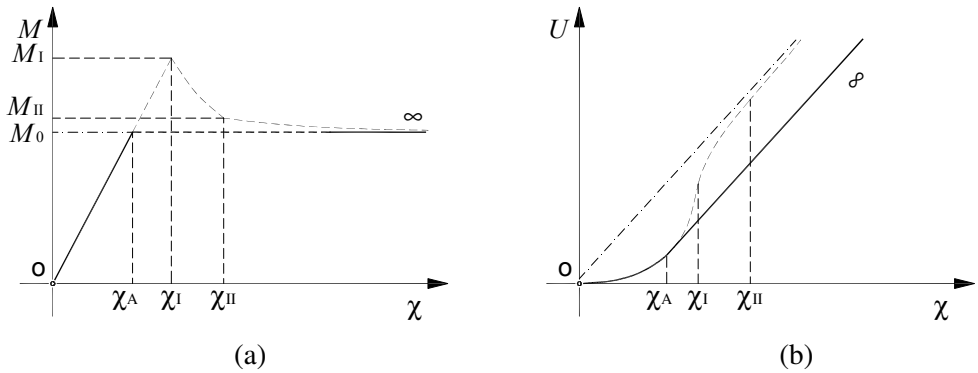

Figure 16. Equilibrium configuration path for case (e) of Figure 11: (a) M-χ relationship, (b) U-χ relationship.

In conclusion, when Equation (1) holds, the $\bar{M}$-δ relationship takes the form

$$\bar{M} = \begin{cases} M(8\delta/l^2), & \delta \le \delta_{\mathrm{A}} = \chi_{\mathrm{A}} l^2/8, \\ M_{\mathrm{M}}, & \delta > \delta_{\mathrm{A}}. \end{cases} \tag{28}$$

It is important to remark that with a process similar to a phase transition when the moment approaches M_0, the strain is instantaneously localized at some point of the beam axis under the form of a concentrated rotation. At that point the curvature increases infinitely, and the corresponding kinematic characterization is analogous to the nucleation of a perfectly plastic hinge. One of the surprising results of this analysis is the predicted $\bar{M}$ versus δ response of Equation (28) matches surprisingly well with the diagrams of Figure 1. In particular, the plastic *plateau* has to be associated with the formation of a plastic hinge which may indefinitely increase the value of the sag δ while keeping fixed the value of the bending moment $\bar{M}$. Moreover, the apparent transition from an upper to a lower yield point in some of the diagrams of Figure 1 may be associated with the attainment of metastable equilibrium states which touch those points in the first linear elastic branch of Figure 15, above the threshold value $M = M_0$.

A similar response can be obtained when the bending moment-curvature relationship is of the type indicated in parts (d) or (e) of Figure 11. The main difference with the previous case (c) is that now

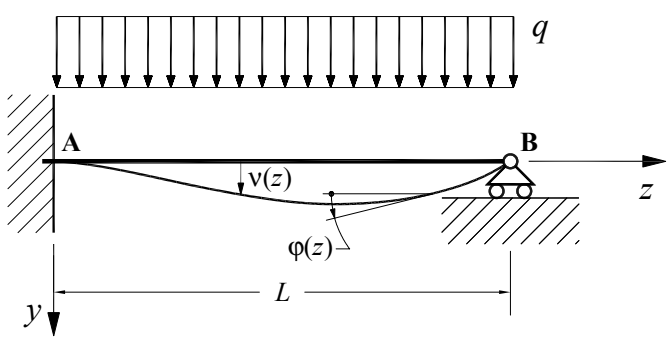

Figure 17. The propped cantilever layout.

there is no strain hardening branch for $\chi \geq \chi_{\mathrm{I}}$. Therefore, by Equation (23), stable equilibrium states can only attain the curvature interval $(\chi, \chi_{\mathrm{A}})$ when $\bar{M} < M_0$. Strain localization occurs at $\bar{M} = M_0$ and neither M_{I} nor M_{II} can be attained (see Figure 16). The form of the energy minimizers is analogous to that expressed in Equation (28).

5. The propped cantilever

To discuss a statically undetermined structure, let us consider the propped cantilever of Figure 17 under the uniform transverse load q. Such a problem has been already recorded in [Royer-Carfagni 2001; Del Piero 2003] for a particular form of a moment-curvature relationship, analogous to that of part (e) of Figure 11, but now the analysis is extended to the remaining cases of that figure. Obviously, if the material response is symmetric in tension and compression, the beam M-χ response is symmetric when the bending moment changes its sign. As a result, the properties of Figure 11 are extended symmetrically with respect to the origin in order to account for this possibility.

Let us briefly recall the main equations of [Royer-Carfagni 2001]. Keeping the notation of Section 4, and once more taking the rotation φ as the independent variable, the functional to be minimized is $\Pi[\varphi]$ of Equation (11) with $W(0) = W(L) = 0$. Using Equations (5) and (10), the boundary conditions $v(0) = v(L)$ give again Equation (12), to which the additional condition $\varphi(0) = 0$ has to be applied. If $\varphi^*(z) \in BV : [0, L] \to \mathbb{R}$ is a minimizer of $\Pi[\varphi]$, then considering the variation $\varphi^* + \varepsilon\psi$ with ψ satisfying Equation (13), one obtains again Equation (14) subject to the additional restriction $\psi(0) = 0$.

We now consider particular variations. First, let $d\psi = d\psi_a$, $d\psi_s = d\psi_d = 0$. Defining the bending moment $M^*(z)$ as in Equation (16), the first variation condition (15) gives, after an integration by parts analogous to Equation (17), the condition

$$d\Pi[\psi] = \int_0^L M^*(z)\psi_a'(z)dz + \int_0^L T(z)\psi_a(z)dz = \big[M^*(z)\psi_a(z)\big]_{z=0}^{z=L} + \int_0^L \Big(-\frac{d}{dz}M^*(z) + T(z)\Big)\psi_a(z)dz = 0.$$

Since the sign of ψ_a is not restricted and $\psi_a(0) = 0$, this is satisfied if and only if

$$M^*(L) = 0, \qquad -M^{*\prime}(z) + T(z) = \text{const.} \tag{29}$$

Evaluation of Equation $(29)_2$ at $z = 0$ gives $C = -M^{*\prime}(0) + T(0)$ or equivalently, using Equation (4), $C = -M^{*\prime}(0) + C_1$, where C_1 represents the vertical reaction at the clamped section A, considered positive if upwards oriented. Without loss of generality, assuming $C_1 = M^{*\prime}(0)$ gives $C = 0$. Then from Equations (4) and $(29)_2$, the equilibrium equations may be written as

$$-M^{*\prime}(z) + T(z) = 0,\ T(z) = M^{*\prime}(0) - \int_0^z q(t)dt. \tag{30}$$

As a second case consider the variation $d\psi = d\psi_a + d\psi_s$, $d\psi_d = 0$. Defining J_+, J_-, and J_0 as in Equation (21), condition (15) yields

$$\begin{aligned}\int_0^L M^*(z)\psi_a'(z)dz + M_0\left(\int_{J_+} d\psi_s - \int_{J_-} d\psi_s + \int_{J_0} |d\psi_s|\right) + \int_0^L T(z)(\psi_a+\psi_s)dz \\ = \left[M^*(z)\psi_a(z)\right]_{z=0}^{z=L} + M_0\left(\int_{J_+} d\psi_s - \int_{J_-} d\psi_s + \int_{J_0} |d\psi_s|\right) + \int_0^L T(z)\psi_s(z)dz \\ = \left[M^*(z)\big(\psi_a(z)+\psi_s(z)\big)\right]_{z=0}^{z=L} + M_0\left(\int_{J_+} d\psi_s - \int_{J_-} d\psi_s + \int_{J_0} |d\psi_s|\right) - \int_0^L M^*(z)d\psi_s \\ = M_0\left(\int_{J_+} d\psi_s - \int_{J_-} d\psi_s + \int_{J_0} |d\psi_s|\right) - \int_0^L M^*(z)d\psi_s \geq 0,\end{aligned}$$

where we have integrated by parts, used Equation $(30)_1$, and in the last line used the fact that $\psi_a(0) + \psi_s(0) = 0$ and $M^*(L) = 0$. Because of the arbitrariness of $d\psi_s$, this again yields condition (23).

Finally, assume a perturbation $d\psi = d\psi_a + d\psi_d$, $d\psi_s = 0$, with ψ_d of the form (24). If $[\![\varphi^*]\!](z_0) = 0$,

$$\int_0^L M^*(z)\psi_a'(z)dz + \int_0^L T(z)\big(\psi_a(z)+\psi_d(z)\big)dz + M_0\big|[\![\psi_d]\!](z_0)\big| \geq 0,$$

which, in view of Equation (30), gives

$$\begin{aligned}\left[M^*(z)\psi_a(z)\right]_{z=0}^{z=L} + \int_0^L \big(-M^*(z)+T(z)\big)\psi_a dz + \left[M^*(z)\psi_d(z)\right]_{z=0}^{z=L} - \int_0^L M^*(z)d\psi_d + M_0\big|[\![\psi_d]\!](z_0)\big| \\ = -M^*(z_0)[\![\psi_d]\!](z_0) + M_0\big|[\![\psi_d]\!](z_0)\big| \geq 0,\end{aligned}$$

and, consequently, the condition $-M_0 \leq M^*(z_0) \leq M_0$. Otherwise, if $[\![\varphi^*]\!](z_0) \neq 0$, one obtains

$$\begin{aligned}\int_0^L M^*(z)\psi_a'(z)dz + \int_0^L T(z)\big(\psi_a(z)+\psi_d(z)\big)dz + M_0\big([\![\psi_d]\!](z_0)\big)\mathrm{sgn}\big([\![\varphi^*]\!](z_0)\big) \\ = -M^*(z_0)[\![\psi_d]\!](z_0) + M_0\big([\![\psi_d]\!](z_0)\big)\mathrm{sgn}\big([\![\varphi^*]\!](z_0)\big) \geq 0,\end{aligned}$$

and, since $[\![\psi_d]\!](z_0)$is arbitrary, condition (25) follows.

The complete characterization of minimizers of the energy functional (11) again requires the second variation inequality (26) and the additional condition coming from the relaxed energy functional (27), that is, the beam curvature $\chi^*(z) \equiv \varphi_a^{*\prime}(z)$ can only attain those values at which U and its lower convex envelope U^{**} coincide.

The detailed derivation of the solution follows that in [Royer-Carfagni 2001; Del Piero 2003]. The starting point is the equilibrium equation $(30)_1$. Considering Equation (4) from which we have $T(z) = qz + C_1$, the differential equation $(30)_1$ can be easily integrated and, by introducing the natural condition $M^*(L) = 0$, it provides the expected parabolic dependence of M^* upon z, that is,

$$M^*(z) = \tfrac{1}{2}q(L^2 - z^2) - C_1(L - z). \tag{31}$$

However, because of Equation (23), M^* can take values only within the admissible range $[-M_0, M_0]$. Such a state coincides with the equilibrium states of a properly defined elastic-perfectly plastic beams, for

which the plastic *plateau* is defined by the horizontal asymptotes of the M-χ curve. We notice that, due to the parabolic dependence of M^* on z, the first two equations of (23)) exclude the presence of plastic zones of finite length along the beam, so that if a plastic deformation occurs, it has to be concentrated at isolated points. In addition, condition (25) at the jump points of φ^* is analogous to that associated with a plastic hinge in the classical sense. Let us then consider, more in detail, the various possibilities.

Consider first the strain hardening M-χ law of part (a) of Figure 11. Assume that the load q and the constant C_1 in Equation (31) are such that $-M_0 < M^*(z) < M_0$. Then, by Equation (23) the rotation field $\varphi^*(z)$ is absolutely continuous, that is, $\varphi_s^*(z) = \varphi_d^*(z) \equiv 0$, and the corresponding curvature $\chi^*(z) \equiv \varphi_a^{*\prime}(z)$ can be found from the assumed M-χ constitutive relationship with Equation (31), as a function of C_1. The value of the constant C_1 is found by imposing Equation (12) and the boundary condition $\varphi(0) = 0$, and checking *a posteriori* that indeed $-M_0 < M^*(z) < M_0$. If the applied load q is gradually augmented, using the aforementioned procedure there will be a value of q such that $|M^*(z)|$ reaches first the threshold value M_0 at some point, say z_R, usually coinciding with the constrained extremity A of Figure 17. However, before reaching such a value, the beam curvature becomes infinitely large in a neighborhood of such a point. Further increasing the load q, the bending moment cannot increase any more at z_R, but the effect of the resultant rotation is that of producing a redistribution of the bending moments along the beam axis. Eventually, the threshold value M_0 is reached at a second point; infinitely large deflection of the beam may now occur because of the formation of a collapse mechanism.

As the second case, let the M-χ relationship be the one of part (b) of Figure 11. When $|M^*| < M_{\mathrm{II}}$, the rotation field $\varphi^*(z)$ and the value of the constant C_1 in Equation (31) can be found as already discussed. If q is further augmented, then in a certain portion of the beam axis $M_{\mathrm{II}} < |M^*| < M_{\mathrm{M}}$, being $M = M_{\mathrm{M}}$ the Maxwell line as part (a) of Figure 14. In this portion there are three values of the curvature that may correspond to the same value of the sectional bending moment, but minimizers of the energy can only take values on the first linear branch, that is, $|\chi^*| < \chi_{\mathrm{A}}$ because on this branch only the strain potential U of Equation (11) and its lower convex envelope U^{**} of Equation (27) coincide. Increasing q, then at some section, say again z_R, $|M^*(z_R)| = M_{\mathrm{M}}$. It is well known [Ericksen 1991] that in this case, analogously to a stress driven test, the beam curvature $|\chi^*(z_R)|$ jumps from the value χ_{A} to the value χ_{B} along the Maxwell line of part (a) of Figure 14. Increasing q, the bending moment also increases, but the beam curvature can never attain values in the interval $(\chi_{\mathrm{A}}, \chi_{\mathrm{B}})$. In other words, the moment-curvature relationship is that corresponding to the points where U and its lower convex envelope U^{**} coincide, represented as well in part (b) of Figure 14. Eventually, like the previous cases, Equation (25) tell us that concentrated rotations may develop at those sections where $|M^*|$ approaches M_0, but only after the beam curvature has reached very large uniform curvatures. The beam collapses when the threshold value M_0 is reached at two distinct sections of the beam.

When the M-χ relationship is that of part (c) of Figure 11, the rotation field $\varphi^*(z)$ and the constant C_1 in Equation (31) can be found as in the previous cases provided the load q is so small that $|M^*(z)| < M_{\mathrm{II}}$ for all $z \in (0, L)$, that is, when one and only one value of the beam curvature corresponds to each value of the bending moment. If q is increased so that $M_{\mathrm{II}} \le |M^*(z)| \le M_0$ for some z, then it is possible to find equilibrium states for which the absolute value of the beam curvature takes two distinct values, one in the interval $(\chi_{\mathrm{I}} M_{\mathrm{II}}/M_{\mathrm{I}}, \chi_{\mathrm{I}} M_0/M_{\mathrm{I}})$, that is, on the first linear elastic branch, and the other in $(\chi_{\mathrm{II}}, +\infty)$, both corresponding to the same value of the bending moment. Again, the possibility of attaining the strain softening branches is ruled out by the second variation condition (26). Moreover, consideration of the

relaxed energy (27), represented in this case in part(b) of Figure 15, implies that only the linear elastic branch can be attained by minimizers, because if $|\chi^*(z)| \in (\chi_{\mathrm{II}}, +\infty)$ then $U(\chi^*(z)) \neq U^{**}(\chi^*(z))$.

The process of formation of a plastic hinge deserves some comments (see [Royer-Carfagni 2001] for more details). Let us assume the beam is progressively loaded. Eventually, the bending moment approaches the limit thresholds M_0 (or $-M_0$) at some points. A further increase of q involves the instantaneous formation of a concentrated rotation, that is, the point representative of M and χ immediately reaches an infinite curvature corresponding to the point at infinity of the horizontal asymptotes of part (c) of Figure 11.

Indeed, neither the softening branches of the moment-curvature relationship nor bending moments in absolute value greater than M_0 are accessible via deformation paths made of stable equilibrium configurations. The beam collapses when the threshold value M_0 is reached at two distinct sections of the beam.

The beam response is very similar to the one just presented when the bending moment versus curvature relationship is of the type indicated in parts (d) or (e) of Figure 11 As discussed in Section 4, the main difference from case (c) is that now there is no strain hardening branch for $\chi \geq \chi_{\mathrm{I}}$. Therefore, by Equation (23) stable equilibrium states can only attain the curvature interval $(\chi, \chi_{\mathrm{A}})$ when $|M^*(z)| < M_0$. Strain localization occurs when $|M^*(z)| = M_0$ at a certain cross section; the value of the bending moment remains fixed at that section, while concentrated rotations are allowed. When q is further increased, this produces a redistribution of the bending moment along the beam axis until, eventually, M_0 is reached at another cross section and we achieve collapse.

6. Discussion and conclusions

The main result of this work consists in having observed that the notion of plastic hinge, usually referred to as an approximate or technical model in the classical plastic methods of structural analysis may be, as a matter of fact, more accurate than traditionally reputed. In the classical approach, when the material is modeled to be elastic-perfectly plastic and cross sections are assumed to remain planar in the deformation, the bending moment M is a monotonically increasing function of the beam curvature χ, asymptotically approaching, but never reaching, the full plastic moment M_0 as $\chi \to \infty$. Ingenious solution methods, such as the approach by Neal and Symonds in limit analysis [Neal 1963] have been developed under the simplifying assumption that the bending moment remains a linear function of the beam curvature up to the attainment of the full plastic moment, at which strain localization under the form of concentrated rotations of the beam axis may indefinitely occur; this is the so-called plastic hinge model. Traditionally, such methods are considered approximate since the transitory stage when the cross section is only partially yielded is neglected.

On the other hand, here we have shown that a response that matches the static-kinematic response of the plastic hinge model can be reproduced by maintaining the most classical Bernoulli–Navier hypothesis, that is, that cross sections remain planar in the deformation, but simply considering the stress jump from an upper to a lower yield point in the material stress-strain constitutive law. Indeed, such a jump is well evident in strain driven experimental tests [Froli and Royer-Carfagni 1999] and is responsible for the orderly formation of Lüder's bands [Froli and Royer-Carfagni 2000]. This jump is usually neglected in the elastic-plastic technical theories, but once it is considered, the moment-curvature relationship,

deduced under the same hypotheses of the classical theories of beams, exhibits a strain-softening branch, while the associated flexural strain potential becomes nonconvex and with oblique asymptotes. The nonconvex character of the potential, together with its linear growth at infinity, are sufficient to provoke a phenomenon presenting a strict similarity with a phase transition in the classical thermodynamic sense within the solid state itself: when a threshold value, coinciding with the value of the full plastic moment, is approached, the beam curvature exhibits a sudden transition. In particular, the beam cross section immediately passes from a state where it is completely elastic to a state where it is completely plasticized, and concentrated rotation may indefinitely occur while the cross sectional bending moment remains constant. In other words, the response predicted upon considering the dichotomy between the upper and lower yield points is surprisingly similar to that referred to as approximate in the technical theories. It should be recalled that the pioneering experimental observations by Nakanishi et al. [1934] seemed to confirm the approximate rather than the ideal response. As such, one may wonder why the results of such tests have been completely forgotten and are not mentioned, to the authors' knowledge, in the majority of famous treatises.

Unfortunately, the present analysis is to some extent limited by the variational approach, which presupposes the hypothesis of reversibility of deformation proper of holonomic plasticity, that is, inelastic unloading can only occur along the same loading path so that the possibility of irreversible unloading, following a path possibly different from the first loading branch, is ruled out. Thus, this approach is certainly not exhaustive and, in a certain sense, even unrealistic. Nevertheless, it certainly greatly facilitates the search of stable equilibrium configurations because they can be investigated as energy minimizers. For this goal recent results in the calculus of variations on space of functions allowing for discontinuities have been conveniently used. On the other hand, consideration of irreversible unloading would require a much more complicated treatment, at least from a mathematical point of view. In any case, although unloading remains the essential aspect of the problem on the side of the localizing damage band, for the case of stable bifurcation (at increasing load) it certainly plays no role for the initial postbifurcation response.

A definite attempt to compare the proposed theory with the experimental observations is still lacking at this stage. Unfortunately, the details of the experimental studies by Nakanishi have not been recorded in the literature so that, in order to investigate the process leading to the strain localization at the mesoscopic scale, an ad hoc experimental campaign is still needed. In particular, it will be important to evaluate the actual width of the plastic *hinge* in order to interpret the sectional (mesoscopic) consequences of strain localization. At the present time the theory seems to suggests that the thickness of the beam cross section may be considered the characteristic length scale of the elastic-plastic transition, but this is certainly a consequence of the orderly formation, at the microscale, of slip (Lüder) bands in a neighborhood of the yielded cross sections. The relationship between the complex phenomena occurring at the meso and microscale and their consequences in the macroscopic interpretation of the proposed theory are presently under investigation and will be the subject of further work.

Another possible criticism could be that the strain hardening branch in the stress-strain response, though well evident in the experiments, is not considered. The material is consequently assumed to be able to withstand indefinitely large strain at constant stress. However, our main goal here has been to show the (quite surprising in our opinion) consequences on the gross structural response of considering just a small stress jump in the constitutive relationship, while maintaining all the other hypotheses of the

classical structural technical theories. Indeed, it is the stress jump from the upper to the lower yield point that induces the peculiarities of the strain energy, that is, its nonconvexity and linear growth at infinity, and it is precisely this that allows for the possibility of sudden discontinuities in the rotation of the beam axis, with a process similar in kind to a phase transition.

References

[Buttazzo 1989] G. Buttazzo, *Semicontinuity, relaxation, and integral representation in the calculus of variations*, Pitman research notes in mathematics **207**, Longman, 1989.

[Cottrell 1953] S. Cottrell, Alan Haward, *Dislocations and plastic flow in crystals*, Claredon Press, Oxford, 1953.

[Del Piero 2003] G. Del Piero, "Structured deformation in plasticity", in *Proceedings of 16th AIMETA Congress*, Ferrara, 2003. In CD-ROM.

[Dunn and Fosdick 1980] J. E. Dunn and R. L. Fosdick, "The morphology and stability of material phases", *Arch. Ration. Mech. An.* **74**:1 (1980), 1–99.

[Ericksen 1975] J. L. Ericksen, "Equilibrium of bars", *J. Elasticity* **5**:3-4 (1975), 191–201.

[Ericksen 1991] J. L. Ericksen, *Introduction to the thermodynamics of solids*, Chapman and Hall, London, 1991.

[Froli and Royer-Carfagni 1999] M. Froli and G. Royer-Carfagni, "Discontinuous deformation of tensile steel bars: experimental results", *J. Eng. Mech. ASCE* **125**:11 (1999), 1243–1250.

[Froli and Royer-Carfagni 2000] M. Froli and G. Royer-Carfagni, "A mechanical model for elastic-plastic behavior of metallic bars", *Int. J. Solids Struct.* **37**:29 (2000), 3901–3918.

[James and Fosdick 1981] R. James and R. L. Fosdick, "The elastica and the problem of pure bending for a nonconvex stored energy function", *J. Elasticity* **11**:2 (1981), 165–186.

[Kolmogorov and Fomin 1975] A. N. Kolmogorov and S. V. Fomin, *Introductory real analysis*, Dover, New York, 1975.

[Müller and Villaggio 1977] I. Müller and P. Villaggio, "A model for an elastic-plastic body", *Arch. Ration. Mech. An.* **65**:1 (1977), 25–56.

[Nakanishi et al. 1934] F. Nakanishi, M. Ito, and K. Kitamura, "On the yield point of mild steel beams under uniform bending", *ARIR* **8**:104 (1934), 273–290. Also in *Selected papers by F. Nakanishi*, Department of Aeronautics, University of Tokyo Press, 1966.

[Neal 1963] B. G. Neal, *The plastic methods of structural analysis*, Wiley, New York, 1963.

[Royer-Carfagni 2001] G. Royer-Carfagni, "Can a moment-curvature relationship describe the flexion of softening beams?", *Eur. J. Mech. A Solid* **20**:2 (2001), 253–276.

[Truskinovsky 1996] L. Truskinovsky, "Fracture as a phase transition", pp. 322–332 in *Contemporary research in the mechanics and mathematics of materials*, edited by R. C. Batra and M. F. Beatty, CIMNE, Barcelona, 1996.

Received 19 Jul 2006. Accepted 13 Feb 2007.

GIANNI ROYER-CARFAGNI: gianni.royer@unipr.it
Dipartimento di Ingegneria Civile, dell'Ambiente, del Territorio e Architettura, Università di Parma, Parco Area delle Scienze 181/A, I 43100 Parma, Italy

GIOVANNI BURATTI: g.buratti@ing.unipi.it
I.T.C.G. Campedelli, Castelnuovo di Garfagnana, Lucca, Italy

and

Dipartimento di Ingegneria Strutturale, Università di Pisa, 56126 Pisa, Italy